

Triplet Supercurrents in Half Metals: the Role of Disorder

Matthias Eschrig and Tomas Löfwander

*Institut für Theoretische Festkörperphysik and DFG-Center for Functional Nanostructures,
Universität Karlsruhe, D-76128 Karlsruhe, Germany*

(Dated: December 4, 2006)

A Josephson supercurrent between two singlet superconducting electrodes separated by an extended region of half-metallic CrO_2 has been recently observed. Since in a half metal only electron pairs with equal spins can carry a supercurrent, there is a conversion from singlet to triplet currents at the interface. The conversion mechanism remains, however, unclear. Another unresolved issue is the symmetry of superconducting correlations in ferromagnets depending on the degree of disorder. In our work we address both problems. We introduce a conversion mechanism based on a broken spin-rotation symmetry around the magnetization axis of the half metal. We show that in the diffusive case the supercurrent is dominated by the product of odd-frequency s -wave and even-frequency p -wave pairing amplitudes, whereas in the ballistic regime the admixture of other components becomes relevant. We study the entire crossover from the ballistic to the diffusive regime.

Half-metallic ferromagnets have great potential in the field of spintronics as sources of spin-polarized electric currents. Remarkably, they show conducting or insulating behavior depending on the direction of the electron spin. Since only a few such half metals are known, among them $\text{La}_{2/3}\text{Ca}_{1/3}\text{MnO}_3$ [1] and CrO_2 [2], their characterization has attracted great attention. Half metals, when contacted with other materials such as superconductors, can also be used as well controlled test-laboratories to study the interplay between different types of orders.

Recently, Keizer *et.al* [2] reported a Josephson supercurrent between two singlet superconducting electrodes (NbTiN) separated by a wide region of CrO_2 . In a half metal only conduction electrons with equal spin can be paired, since the other spin species is insulating. Currently, the mechanism involved in the conversion process between singlet Cooper pairs $(|\uparrow\downarrow\rangle - |\downarrow\uparrow\rangle)/\sqrt{2}$ and equal spin pairs $|\uparrow\uparrow\rangle$ at the interfaces between the materials remains highly controversial. In the same experiment [2] a second, seemingly unrelated, observation was made, namely the presence of a homogeneous biaxial magnetic asymmetry in the CrO_2 film (see Fig. 1).

The symmetries of the relevant pairing correlations mediating the triplet supercurrent and their dependence on the amount of disorder is currently debated. It is claimed [3, 4] that the main source of the triplet Josephson current in diffusive ferromagnets is odd-frequency s -wave pairing amplitudes. On the other hand, it has been shown that in clean half metals also p -wave triplet pairing amplitudes are important [5]. The samples in experiment [2] are moderately disordered, and a detailed theoretical study of the crossover from the ballistic to the diffusive regimes is required.

Here we report an extensive analytical and numerical investigation of the Josephson effect in the hybrid structure shown in Fig. 1 and present results for an arbitrary concentration of impurities in the materials, thereby clar-

ifying the symmetry properties of the superconducting correlation functions involved. We link the mechanism for the current conversion to a broken spin-rotation symmetry around the magnetization axis \mathbf{M} in the half metal. We argue that the second observation in experiment [2] of a biaxial magnetic asymmetry can be directly related to the conversion mechanism of the singlet supercurrent to the triplet supercurrent.

The mechanism we propose leads to a natural explanation of several findings of the experiment [2]: (i) hysteretic shifts of the equilibrium phase difference over

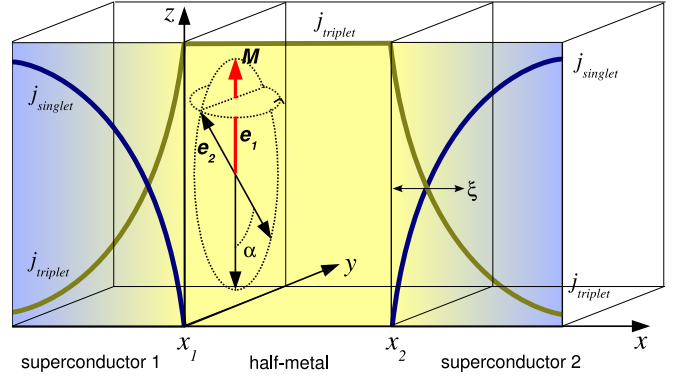


FIG. 1: Conversion between singlet and triplet supercurrents. The setup consists of two singlet superconductor banks separated by a half-metallic ferromagnetic CrO_2 layer with a magnetization vector \mathbf{M} aligned along the easy axis \mathbf{e}_1 . Spin-rotation symmetry around \mathbf{M} is broken by the simultaneous presence of the second easy axis \mathbf{e}_2 . As a consequence, there is a conversion from a supercurrent of singlet Cooper pairs (j_{singlet} , blue lines) in the superconductors to a supercurrent of triplet Cooper pairs in the half metal (j_{triplet} , yellow line). The conversion takes place in the superconductors in a layer extending about a superconducting coherence length from the interface, as illustrated by the shading from blue to yellow.

the junction depending on the magnetic pre-history; (ii) Josephson junctions involving half metals are π -junctions after subtraction of the hysteretic shifts; (iii) sample-to-sample fluctuations in the magnitude of the critical current.

We show that in moderately disordered half metals the supercurrent is carried predominantly by odd-frequency s -wave and d -wave amplitudes, multiplied with even frequency p -wave and f -wave amplitudes. In the diffusive limit the supercurrent is dominated by the product of the s -wave and the p -wave amplitudes. We find that a peak in the temperature dependence of the critical current, previously predicted for clean half metals [5], is a robust feature also for disordered half metals.

The Josephson junction we study, shown in Fig. 1, consists of a half metal extending from x_1 to x_2 , sandwiched between two singlet superconductors. When a phase difference $\chi_2 - \chi_1$ exists between the superconducting order parameters, an exotic form of Josephson effect occurs: a singlet supercurrent, j_{singlet} (blue in Fig. 1), is converted to an equal-spin triplet supercurrent, j_{triplet} (yellow in Fig. 1), within an interface layer extending about a superconducting coherence length into the electrodes. The equal-spin triplet supercurrent flows through the half-metallic material, while the singlet part is completely blocked. The sum of the singlet and triplet currents is constant, obeying the continuity equation.

The conversion process between the singlet and equal-spin triplet supercurrents is triggered by two important phenomena taking place at the interface: (i) spin mixing and (ii) breaking of spin-rotation symmetry with respect to the magnetization axis \mathbf{M} in the half metal. Spin-mixing is the result of different scattering phase shifts that electrons with opposite spin acquire when scattered (reflected or transmitted) from an interface [6]. It results from either a spin-polarization of the interface potential, or differences in the wavevector mismatches for spin up and spin down particles at either side of the interface, or both. It is a robust and ubiquitous feature for interfaces involving strongly spin-polarized ferromagnets.

Broken spin-rotation symmetry leads to spin-flip processes at the interfaces. Its origin is more subtle and deserves special attention. Here we propose a mechanism that applies to biaxial ferromagnets with local magnetic moments coupled to itinerant electrons. Indeed, the fully spin-polarized CrO_2 films used in the experiment [2] have been shown to be homogeneously biaxial [10]. At the interfaces with the superconductors, the local moments are expected to show a certain degree of disorder for two reasons. First, the coordination number is lowered by the broken translation symmetry at the interface which leads to enhanced fluctuations in the direction of the local moments from that in the ordered phase. Secondly, structural disorder leads to vacancies in the lattice of moments. The exact microscopic distribution of local moments at the interface is not important for superconduct-

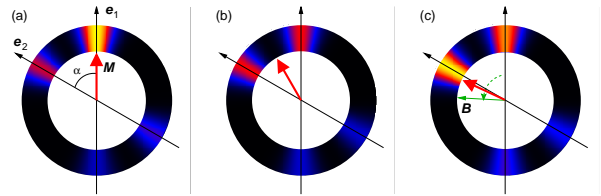


FIG. 2: **Breaking of spin-rotation symmetry at the interface.** (a) Misaligned local moments at the interface involving a magnetic material with biaxial anisotropy prefer the second easy axis e_2 , leading to an explicitly broken spin rotation symmetry around the magnetization axis (here parallel to the easy axis e_1). (b) If the magnetization is pointing exactly between the two easy axes, spin-rotation invariance is possible. (c) However, hysteresis effects usually prevent such a situation for any orientation of the magnetization vector.

ing phenomena, since Cooper pairs are of the size of the coherence length ξ which is much larger than the atomic scale. It is, however, important for the effective interface scattering matrix, as it can lead to spin-flip terms if the directional distribution of the local moments breaks the spin-rotation symmetry around \mathbf{M} .

We propose that the presence of two easy axes with relative angle α leads to a non-trivial distribution of the moments at the interface, where a majority of the moments are pointing along the magnetization axis of the bulk half metal but with a significant number of moments misaligned but preferably along the second easy axes. For example, the distribution in Fig. 2(a) leads to a model where the spin-rotation symmetry around \mathbf{M} (satisfied in the bulk material) is broken near the interface within a few atomic layers.

To quantify the above discussion, we employ a simple model that is formulated in terms of an interface scattering matrix, which connects incoming to outgoing waves in the asymptotic regions [5],

$$\hat{\mathbf{S}} = \begin{pmatrix} e^{\frac{i}{2}\vartheta} & 0 & t_{\uparrow\uparrow}e^{i(\vartheta_{\uparrow\uparrow}+\frac{\vartheta}{4})} \\ 0 & e^{-\frac{i}{2}\vartheta} & t_{\downarrow\uparrow}e^{i(\vartheta_{\downarrow\uparrow}-\frac{\vartheta}{4})} \\ \overline{t_{\uparrow\uparrow}e^{-i(\vartheta_{\uparrow\uparrow}-\frac{\vartheta}{4})}} & \overline{t_{\downarrow\uparrow}e^{-i(\vartheta_{\downarrow\uparrow}+\frac{\vartheta}{4})}} & -1 \end{pmatrix}. \quad (1)$$

Here, $t_{\uparrow\uparrow}$ and $t_{\downarrow\uparrow}$ are transmission amplitudes from the two superconducting spin bands to the conducting half-metallic spin- \uparrow band, and ϑ , $\vartheta_{\uparrow\uparrow}$, and $\vartheta_{\downarrow\uparrow}$ are spin-mixing angles. This scattering matrix is appropriate for the tunneling limit, in which case its reflection amplitudes have unity modulus. The extra phases $\pm\vartheta/4$ ensure unitarity of $\hat{\mathbf{S}}$ up to linear order in the transmission amplitudes. For definiteness, we have chosen the spin quantization axis in the half metal along \mathbf{M} , and in the superconductor such that the reflection amplitude of the scattering matrix is diagonal in the tunneling limit. In a system with spin rotation invariance around \mathbf{M} these two quantization axes coincide. This is, however, in general not the case if spin rotation symmetry around \mathbf{M} is broken.

The presence of the spin-flip terms $t_{\downarrow\uparrow}e^{\pm i\vartheta_{\downarrow\uparrow}}$ in the scattering matrix Eq. (1) is a direct consequence of the broken spin-rotation symmetry around \mathbf{M} at the interface.

In the following we calculate the Josephson current through the junction in leading order in $t_{\uparrow\uparrow}$, $t_{\downarrow\uparrow}$, and ϑ . As corrections to the singlet order parameter Δ arise in second order in ϑ , we can neglect the suppression of Δ near the interfaces. In this case Anderson's theorem [11, 12] holds and Δ is also insensitive to impurity scattering. For simplicity we consider the case of equal gap magnitudes in the two superconductors, $\Delta_j = |\Delta|e^{i\chi_j}$, for superconductors $j = 1$ and $j = 2$, see Fig. 1.

Due to spin mixing at the interfaces a spin triplet ($S = 1$, $m = 0$) amplitude $f_{t_0j}(x)$ is developed that extends from the interfaces about a coherence length into each superconductor,

$$f_{t_0j}(x) = i\pi|\Delta|e^{i\chi_j}\vartheta_j \frac{|\varepsilon_n|\varphi_{0j}^s(x) + \Omega_n\varphi_{0j}^a(x)}{\Omega_n^2}, \quad (2)$$

where $\Omega_n = \sqrt{\varepsilon_n^2 + |\Delta|^2}$. We have separated the influence of the interfaces from that of the impurity disorder in the bulk materials by introducing the real functions $\varphi_{0j}^{s,a}(x)$. The superscript denotes symmetric (s) and antisymmetric (a) components with respect to $\mu = \cos(\theta_p)$, where θ_p is the angle between the Fermi velocity and the x -axis. In the clean limit, $\varphi_{0j}^a(x) = -\frac{\text{sgn}(\mu)}{2}e^{-|x-x_j|/\xi_S|\mu|}$ and $\varphi_{0j}^s(x) = -\varphi_{0j}^a(x)\text{sgn}(\mu\varepsilon_n)$, where $\xi_S = v_S/2\Omega_n$, and v_S is the Fermi velocity in the superconductor. For an arbitrary impurity concentration the φ -functions are modified and must be calculated numerically for each given value of mean free path, as described in the Methods.

Whereas the interface value of $f_{t_0j}^a$ does not change with varying mean free path, the interface value of $f_{t_0j}^s$ increases with decreasing mean free path in the superconductor, ℓ_S , as $1/\sqrt{\ell_S}$ until it reaches values comparable with the singlet amplitude. Their decay length in the superconductors decreases, and changes from $(\xi_S^{-1} + \ell_S^{-1})^{-1}$ in the ballistic limit to $\sqrt{\xi_S\ell_S/3}$ in the diffusive limit (see Supplementary Fig. 1). For definiteness, in the remaining discussion we use for the mean free path in the superconductors $\ell_S = 0.1\xi_0$ with $\xi_0 = v_S/2\pi T_c$.

The singlet-triplet mixing in the surface layers of the superconductors described above, together with the presence of spin-flip tunneling amplitudes, leads to an equal-spin ($m = 1$) pairing amplitude $f_{\uparrow\uparrow}(x)$ in the half metal. We would like to emphasize that it is only the $m = 0$ triplet component derived above that is coupled via the spin-active boundary condition to the $m = 1$ pairing amplitude in the half metal. The singlet components in the superconductor, being invariant under rotations around any quantization axis, is not directly involved in the creation of the triplet in the half metal. A picture of an indirect Josephson effect emerges, therefore, that is mediated by the appearance of the $m = 0$ triplet amplitudes in the superconductor.

In the tunneling limit it is convenient to split the pairing amplitude in the half metal into contributions induced at the left and right interfaces: $f_{\uparrow\uparrow} = f_{\uparrow\uparrow 1} + f_{\uparrow\uparrow 2}$, with momentum-symmetric and antisymmetric components

$$f_{\uparrow\uparrow j}^{s,a}(x) = 2\pi i(t_{\uparrow\uparrow j}t_{\downarrow\uparrow j}\vartheta_j)|\Delta|e^{i\bar{\chi}_j} \frac{|\varepsilon_n|}{\Omega_n^2} \varphi_j^{s,a}(x) \quad (3)$$

where $\bar{\chi}_j = \chi_j - \vartheta_{\uparrow\uparrow j} - \vartheta_{\downarrow\uparrow j}$. Here, like above, we have separated the contributions from the interface scattering matrix and the contributions from the disorder in the half metal by introducing the (real) functions $\varphi_j^{s,a}$.

The Josephson current results from Eq. (16) in Methods,

$$J_x = -J_c \sin(\bar{\chi}_2 - \bar{\chi}_1), \quad (4)$$

where the critical current density is given by

$$J_c = J_0 \frac{T}{T_c} \sum_{\varepsilon_n > 0} \frac{|\Delta|^2 \varepsilon_n^2}{\Omega_n^4} \langle \mu A_1 A_2 (\varphi_2^s \varphi_1^a - \varphi_2^a \varphi_1^s) \rangle. \quad (5)$$

Here, the current unit is $J_0 = 4\pi e v_H N_H T_c$, N_H is the density of states at the Fermi level in the half metal, e is the electron charge, $A_j = (t_{\uparrow\uparrow j}t_{\downarrow\uparrow j}\vartheta_j)$, and $\langle \dots \rangle = \int_0^1 d\mu \dots$. The effective phase on each side j is

$$\bar{\chi}_j = \chi_j - (\vartheta_{\uparrow\uparrow j} + \vartheta_{\downarrow\uparrow j}). \quad (6)$$

Eqs. (4)-(6) describe an exotic Josephson effect in several respects. Eq. (6) is related to the phase dependence of the Josephson effect and can be tested for example by studying the Fraunhofer pattern in a magnetic field. For a half metal, there can be extra phases that lead to shifts of the Fraunhofer pattern [15, 16]. Within our model there are contributions $\vartheta_{\downarrow\uparrow 2} - \vartheta_{\downarrow\uparrow 1}$ and $\vartheta_{\uparrow\uparrow 2} - \vartheta_{\uparrow\uparrow 1}$ to the phases that depend on the microscopic structure of the disordered magnetic moments at the two interfaces. The microstructure can be affected for example by applying a magnetic field that leads to hysteretic shifts of the equilibrium positions depending on the magnetic pre-history. When subtracting the shifts, the junction shows the typical characteristics of a π -junction, [14] as revealed by the minus-sign in Eq. (4). The possibility to manipulate the shifts with an external field yields a way to measure the combination $\vartheta_{\uparrow\uparrow} + \vartheta_{\downarrow\uparrow}$ of the spin-mixing angles. This is important as there have been no experiments to date that give information about the spin-mixing angles. Finally, the critical Josephson current is proportional to the spin-mixing angles ϑ and to the spin-flip rates of the two interfaces. This points to a strong sensitivity of the critical Josephson current to interface properties and is expected to lead to strong sample-to-sample variations. All these findings are in agreement with the experiment [2].

We now proceed with a detailed description of the role of disorder in the materials. Anisotropic superconducting

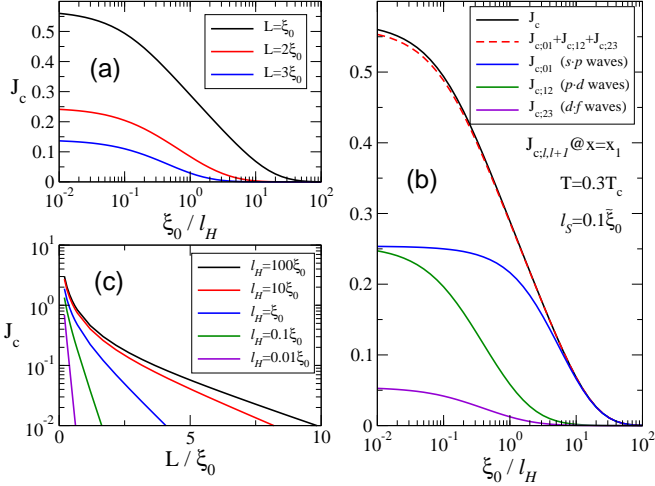


FIG. 3: **Critical Josephson current.** (a) In the crossover from the ballistic to the diffusive limits the critical current J_c is monotonically suppressed. (b) In the crossover region, contributions to the current from higher partial waves ($l \geq 2$, d -wave, f -wave, etc.) of the superconducting Green's function are suppressed. In the diffusive limit the current (black line) is given by a product of s -wave ($l = 0$) and p -wave ($l = 1$) components (the blue line). (c) For given mean free path, J_c is exponentially suppressed for junction lengths large compared with the coherence length ($\xi_c = v_H/2\pi T$ in the ballistic limit and $\xi_d = \sqrt{\xi_c \ell_H/3}$ in the diffusive limit). J_c is given in units of $J_0 A_1 A_2 / 4\pi$. The length unit is $\xi_0 = \xi_c(T_c)$. We assumed an anisotropy of both $t_{\uparrow\uparrow}$ and $t_{\downarrow\downarrow}$ proportional to $|\mu|$.

correlations are sensitive to impurity scattering. From studies of unconventional superconductivity it is known that superconductivity disappears at a critical impurity concentration [13]. This is however not the case for the proximity induced pairing amplitudes studied here. In Fig. 3 we show results for the critical Josephson current as function of the elastic mean free path, normalized to $\xi_0 = v_H/2\pi T_c$. As shown in Fig. 3(a), the critical current is monotonously suppressed for decreasing mean free path, from ballistic (left part of the abscissa in the figure) to diffusive (right part) transport. The suppression is exponential in the diffusive region, with a crossover taking place at a mean free path ℓ_H comparable with the clean limit coherence length $\xi_c = v_H/2\pi T$.

In order to better understand the nature of the crossover we show in Fig. 3(b) the decomposition of the Josephson current into symmetry components. We note that the current is carried by the product of neighboring symmetry components of the functions $\bar{\varphi}_j \equiv A_j \varphi_j$ in Eq. (5), i.e. $J_c = \sum_{l=0}^{\infty} J_{c;l,l+1}$. This can be seen by expanding the pairing amplitudes in Legendre polynomials, $\bar{\varphi}_j(\mu) = \sum_{l=0}^{\infty} P_l(\mu) \bar{\varphi}_{j,l}$, leading to terms of the form $\bar{\varphi}_{2,l} \bar{\varphi}_{1,l+1} - \bar{\varphi}_{1,l} \bar{\varphi}_{2,l+1}$ in Eq. 5, where $l = 0, 1, 2, 3, \dots$ denotes the s -, p -, d -, f -wave etc. pairing components. As all pairing amplitudes involved are spin triplet, the even l amplitudes are odd in frequency while the odd l

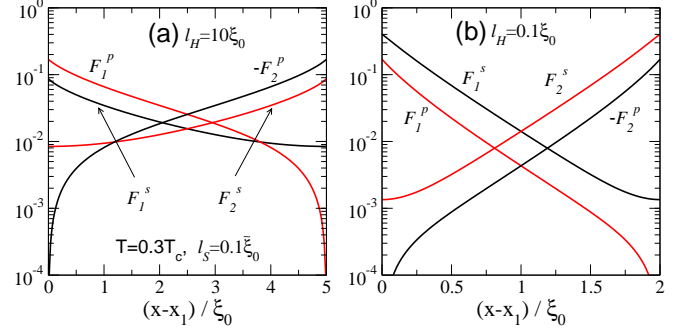


FIG. 4: **Triplet correlation functions in the half metal.** The contribution to the Josephson current from the s -wave triplet equal spin correlation function always enters as a product with the p -wave, with one of the two originating from the left superconductor and the other from the right. For clean half metals, shown in (a), the p -wave component is larger than the s -wave. For more dirty structures, shown in (b), the p -wave component is suppressed compared with the s -wave and the Josephson current is suppressed accordingly. The symmetry components are defined as $F_j^s(x) = T \sum_{\varepsilon_n > 0} \langle f_{\uparrow\uparrow j}(x) \rangle \frac{|\Delta|}{\Omega_n}$, $F_j^p(x) = \frac{1}{3} T \sum_{\varepsilon_n > 0} \langle \mu f_{\uparrow\uparrow j}(x) \rangle \frac{|\Delta|}{\Omega_n}$, plotted in units of $i A_j |\Delta| e^{i \bar{\chi}_j}$. Amplitudes for fixed frequency give a similar picture.

amplitudes are even in frequency [16]. The sum of the first three contributions (red dashed line), composed from the $s \cdot p$ (blue), $p \cdot d$ (green), and $d \cdot f$ (purple) components, amount already to almost the entire current (black line). In the diffusive limit, the current is carried almost exclusively by the product of the even-frequency p -wave and the odd-frequency s -wave pairing amplitudes. The crossover region to ballistic transport is characterized by an onset of contributions from higher order partial waves $l \geq 2$. It is clear from the figure, that for $\ell_H \geq \xi_0$ the diffusive Usadel approximation breaks down.

In Fig. 3 (c) we show for several mean free paths the dependence of the critical current on the junction length L . A rapid exponential suppression of the effect with junction length is observed in the diffusive region, whereas in the moderate disordered region a considerable effect is expected for junction lengths up to 5-10 coherence lengths.

In Fig. 4 we present an analysis of the spatial dependences of the odd-frequency s -wave and even-frequency p -wave pairing amplitudes in the half metal. We show for the ballistic case ($\ell_H = 10\xi_0$) and for the diffusive case ($\ell_H = \xi_0/10$) the pairing amplitudes induced from the left and right interfaces. By multiplying the two black curves with each other and the two red curves with each other, and summing the two contributions, we obtain a quantity related to the $s \cdot p$ contribution to the Josephson current [see Eq. (5)]. For ballistic systems the p -wave amplitudes are larger than the s -wave amplitudes near the interfaces, while the opposite holds for diffusive systems. Note, however, that the amplitudes are

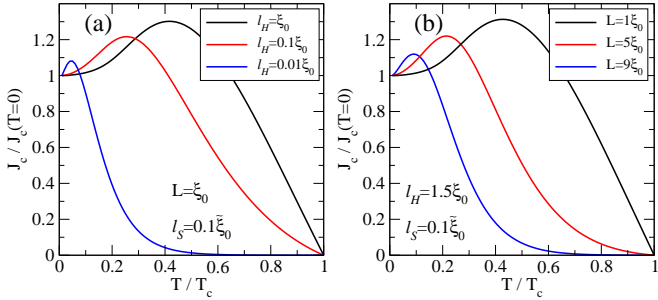


FIG. 5: **Non-monotonic temperature dependence.** (a) The critical Josephson current has a maximum at a low temperature that for a specific junction length [here $L = \xi_0 = \xi_c(T_c)$] depends on the mean free path in the half metal. For $\ell_H > \xi_0$ the peak position roughly coincides with that of the $\ell_H = \xi_0$ curve. The current has been normalized to the zero-temperature value. In (b) we show the normalized current as function of junction length L for a fixed mean free path $\ell_H = 1.5\xi_0$. From (a) and (b) it follows that for diffusive systems the junction becomes effectively long compared with the diffusive limit coherence length, $L = \xi_0 \gg \xi_d(T)$; the current is then dramatically suppressed [see Fig. 3(a)] and the peak is shifted to lower temperatures.

tied to each other through the following general relation between the momentum-antisymmetric and the momentum symmetric parts: $f_{\uparrow\uparrow}^a = -\text{sgn}(\varepsilon_n)\mu\xi_H\partial_x f_{\uparrow\uparrow}^s$, where $\xi_H^{-1} = \ell_H^{-1} + 2|\varepsilon_n|/v_H$. In the diffusive limit, there is an additional relation, $f_{\uparrow\uparrow}^{p\text{-wave}} = -\text{sgn}(\varepsilon_n)\ell_H\partial_x f_{\uparrow\uparrow}^{s\text{-wave}}$. It follows (see Fig. 4) that the *magnitudes* of the amplitudes differ (their ratio depends on the amount of disorder) while the *decay lengths* of the two are always identical, crossing over from the ballistic coherence length $\xi_c = v_H/2\pi T$ to the diffusive coherence length $\xi_d = \sqrt{\ell_H\xi_c/3}$.

Finally, we discuss the influence of disorder on the temperature dependence of the critical current, see Fig. 5. We have normalized all $J_c(T)$ curves to their zero-temperature value. There is a characteristic peak appearing at a temperature below $\sim T_c/2$ as predicted for ballistic systems in Ref. [5]. The origin of the peak is the extra factor $\varepsilon_n^2/\Omega_n^2$ in Eq. (5), that results from the odd-frequency pairing amplitudes on the *superconducting sides* of the interfaces being the sources of the equal spin correlations in the half metal.

In Fig. 5(a) we discuss $J_c(T)$ for mean free paths in the half metal ranging from ballistic to diffusive. Clearly, the peak is observed also in the extreme diffusive case of $\ell_H = \xi_0/100$, but is for a particular junction length L shifted to lower temperatures with decreasing mean free path. Since the peak survives the crossover from the ballistic to the diffusive limits, it serves as a true fingerprint of equal spin triplet correlations in the half metal. The peak is readily measurable experimentally when L is of the order of the coherence length at T_c . For increasing L the peak is shifted to lower temperatures, as shown in Fig. 5(b) for $\ell_H = 1.5\xi_0$. For long junctions

the current has a characteristic exponential temperature dependence above the peak.

Turning to Ref. [2], the low-temperature resistivity of the CrO_2 material of $8.9 \mu\Omega \text{ cm}$ implies a mean free path of $\ell_H \approx 40 \text{ nm}$. From band structure calculations, the Fermi velocity for CrO_2 is $v_H \approx 2.2 \times 10^5 \text{ m/s}$ [17], implying $\xi_0 \approx 27 \text{ nm}$, or $\xi_0/\ell_H \approx 2/3$ (for $T = 0.3T_c$ this gives $\xi_c \approx 90 \text{ nm}$ and $\xi_d \approx 35 \text{ nm}$). The CrO_2 of Ref. [2] is therefore moderately disordered, being in the crossover region in Fig. 3(b), rather than in the clean or diffusive limits. With the typical length of CrO_2 in [2] of $L \approx 300 \text{ nm} \approx 11\xi_0$, we can from Fig. 5(b) predict that if measurements are extended to lower temperatures, or a shorter junction length is used, a peak in $J_c(T)$ should be observed.

In conclusion, we have presented a detailed study of spin-triplet supercurrents through half-metallic ferromagnets. We have pointed out that ferromagnets with biaxial asymmetry are particularly suitable for creating such triplet supercurrents. We have studied in detail the role of disorder and found that the mechanism we propose is robust. We have clarified the symmetries of the pairing amplitudes that determine the Josephson current, and have made predictions that can be tested experimentally. In particular, there is a robust peak in the temperature dependence of the critical Josephson current that signals the involvement of odd frequency pairing amplitudes.

METHODS

We obtain the Josephson current as function of impurity concentration, temperature and junction length using the quasiclassical Green's functions technique [8, 9]. The Green's functions $\hat{g}(\mathbf{p}_F, \mathbf{R}, \varepsilon_n)$ depend on the spatial coordinate \mathbf{R} , Matsubara energy $\varepsilon_n = (2n+1)\pi T$, and the momentum direction on the Fermi surface \mathbf{p}_F . In the superconductors, the propagator \hat{g} is a 4x4 matrix in combined spin and particle-hole space,

$$\hat{g}^S = \begin{pmatrix} g_s + \mathbf{g}_t \cdot \boldsymbol{\sigma} & (f_s + \mathbf{f}_t \cdot \boldsymbol{\sigma})i\sigma_y \\ (\tilde{f}_s + \tilde{\mathbf{f}}_t \cdot \boldsymbol{\sigma}^*)i\sigma_y & \tilde{g}_s + \tilde{\mathbf{g}}_t \cdot \boldsymbol{\sigma}^* \end{pmatrix}, \quad (7)$$

where f_s and \mathbf{f}_t are singlet and triplet pairing amplitudes, g_s and \mathbf{g}_t are spin scalar and spin vector parts of the diagonal Green function, and the vector $\boldsymbol{\sigma} = (\sigma_x, \sigma_y, \sigma_z)$ is composed of Pauli spin matrices. The hole amplitudes are related the particle amplitudes by the symmetry $\tilde{f}(\mathbf{p}_F, \varepsilon_n) = f(-\mathbf{p}_F, \varepsilon_n)^*$. In the half metal, only conduction electrons with spin up exist, and the propagator is a 2x2 matrix in particle-hole space,

$$\hat{g}^H = \begin{pmatrix} g_{\uparrow\uparrow} & f_{\uparrow\uparrow} \\ \tilde{f}_{\uparrow\uparrow} & \tilde{g}_{\uparrow\uparrow} \end{pmatrix}. \quad (8)$$

The propagators are connected at the interfaces via the scattering matrices given in Eq. (1).

The transport equation governing the supercurrent in the heterostructure is given by the Eilenberger equation for the propagator \hat{g} . Impurities are treated in the Born approximation using a life time τ_S of quasiparticles in the superconductor, and a life time τ_H in the half metal. The corresponding mean free paths are $\ell_S = v_S \tau_S$, $\ell_H = v_H \tau_H$, with the Fermi velocities v_S and v_H in the two materials. The equation of motion for the 4x4 Green's function in the superconductors reads,

$$iv_S \mu \partial_x \hat{g} + \left[i\varepsilon_n \hat{\tau}_3 - \hat{\Delta} - \frac{1}{2\pi\tau_S} \langle \hat{g} \rangle, \hat{g} \right] = \hat{0}, \quad (9)$$

where $\mu = \cos(\theta_p)$, θ_p is the angle between the Fermi velocity and the x -axis, $\hat{\tau}_3$ is the third Pauli matrix in particle-hole space, and $\hat{\Delta} = \Delta \hat{1} i \sigma_y$ is the singlet order parameter. The average $\langle \dots \rangle = \int \frac{d\cos(\theta_p) d\varphi_p}{4\pi} \dots$ is over all momentum directions. There is an analogous equation for the 2x2 Green's function in the half metal,

$$iv_H \mu \partial_x \hat{g} + \left[i\varepsilon_n \hat{\tau}_3 - \frac{1}{2\pi\tau_H} \langle \hat{g} \rangle, \hat{g} \right] = \hat{0}. \quad (10)$$

Eqs. (9)-(10) are supplemented with the normalization condition $\hat{g}^2 = -\pi^2 \hat{1}$.

We linearize the above equations for small triplet components in the superconductor (f_{t_0}) and in the half metal ($f_{\uparrow\uparrow}$). The normalization condition is then used to eliminate the diagonal part of \hat{g} in favor of a coupled set of equations for f -functions with positive and negative momentum directions. We decouple the system of differential equations by introducing the new triplet functions φ_0 and φ in Eqs. (2)-(3).

The solutions for the functions $\varphi_{0j}^{s,a}$, appearing in the ansatz (2) for the superconductors, are given by

$$\varphi_{01}^s(x) = \frac{s_\varepsilon}{2} B_{01}(x) + \int_{-\infty}^{x_1} dx' \frac{K_1(x, x')}{2|\mu|\ell_S} \langle \varphi_{01}^s(x') \rangle \quad (11)$$

$$\varphi_{02}^s(x) = \frac{s_\varepsilon}{2} B_{02}(x) + \int_{x_2}^{\infty} dx' \frac{K_2(x, x')}{2|\mu|\ell_S} \langle \varphi_{02}^s(x') \rangle \quad (12)$$

with $s_\varepsilon = \text{sgn}(\varepsilon_n)$, $B_{0j}(x) = e^{-|x-x_j|/\xi_S|\mu|}$, $K_j(x, x') = e^{-|x-x'|/\xi_S|\mu|} + e^{-(|x'-x_j|+|x-x_j|)/\xi_S|\mu|}$, and $\xi_S = v_S/(2\Omega_n + \tau_S^{-1})$ with $\Omega_n = \sqrt{\varepsilon_n^2 + |\Delta|^2}$. The momentum-antisymmetric parts are obtained by using the identity $\varphi_{0j}^a = -\mu s_\varepsilon \xi_S \partial_x \varphi_{0j}^s$.

In the half metal the solutions for $\varphi_j^{s,a}$ are

$$\varphi_j^s(x) = \frac{1}{1 - e^{-2L/\xi_H|\mu|}} \left(\frac{s_\varepsilon}{2} B_j(x) + \int_{x_1}^{x_2} dx' \frac{K(x, x')}{2|\mu|\ell_H} \langle \varphi_j^s(x') \rangle \right) \quad (13)$$

with $\xi_H = v_H/(2|\varepsilon_n| + \tau_H^{-1})$, $L = x_2 - x_1$, $B_1(x) = \varphi_{01}(x_1) (e^{-(x-x_1)/\xi_H|\mu|} + e^{-(L+x_2-x)/\xi_H|\mu|})$, $B_2(x) = \varphi_{02}^s(x_2) (e^{-(x_2-x)/\xi_H|\mu|} + e^{-(L+x-x_1)/\xi_H|\mu|})$, $K(x, x') =$

$e^{-|x-x'|/\xi_H|\mu|} + e^{-(2L-|x-x'|)/\xi_H|\mu|} + e^{-(x+x'-2x_1)/\xi_H|\mu|} + e^{-(2x_2-x-x')/\xi_H|\mu|}$. The momentum-antisymmetric parts are obtained by using the identity $\varphi_j^a = -\mu s_\varepsilon \xi_H \partial_x \varphi_j^s$.

The integral equations (11)-(13) for $\langle \varphi^s(x) \rangle$ are solved by replacing φ on a spatial grid with a piecewise linear function. Exact integration of the resulting expressions reduces the problem to a simple matrix inversion. The angular averages can be performed analytically and lead to exponential integrals. This procedure is necessary because the integration kernel decays on a different length scale compared with φ in the diffusive limit.

The current density in the half metal is given by the diagonal Green's function,

$$J_x(x) = ev_H N_H T \sum_{\varepsilon_n} \langle \mu g_{\uparrow\uparrow}(\mu, \varepsilon_n, x) \rangle \quad (14)$$

where N_H is the density of states at the Fermi level for the conducting spin band in the half metal, and e is the electronic charge. It can be shown from the transport equations (9) and (10) that the current density J_x does in fact not depend on the spatial coordinate, in agreement with the continuity equation that expresses particle conservation.

Using the normalization condition in the half metal, $g_{\uparrow\uparrow}^2 = -\pi^2 + f_{\uparrow\uparrow} \tilde{f}_{\uparrow\uparrow}$, for small triplet amplitudes, one obtains in leading order $g_{\uparrow\uparrow} = -i\pi \text{sgn}(\varepsilon_n) (1 - f_{\uparrow\uparrow} \tilde{f}_{\uparrow\uparrow} / 2\pi^2)$, leading to

$$J_x = \frac{iev_H N_H}{2\pi} T \sum_{\varepsilon_n} \langle \mu f_{\uparrow\uparrow}(\mu, \varepsilon_n, x) \tilde{f}_{\uparrow\uparrow}(\mu, \varepsilon_n, x) \rangle \text{sgn}(\varepsilon_n). \quad (15)$$

It is instructive to decompose the anomalous propagators into their symmetric and antisymmetric part $f_{\uparrow\uparrow}^{s,a}$ with respect to μ . Doing this and using the fundamental symmetries $f_{\uparrow\uparrow}^s(-\varepsilon_n) = -f_{\uparrow\uparrow}^s(\varepsilon_n)$, $f_{\uparrow\uparrow}^a(-\varepsilon_n) = f_{\uparrow\uparrow}^a(\varepsilon_n)$ we arrive at

$$J_x = -\frac{2ev_H N_H}{\pi} T \sum_{\varepsilon_n > 0} \int_0^1 d\mu \mu \text{Im}(f_{\uparrow\uparrow}^s f_{\uparrow\uparrow}^{a*}). \quad (16)$$

Substitution of Eq. (3) into Eq. (16) leads to Eqs. (4)-(6).

To study the symmetry properties of the Josephson current, we expand the pairing amplitudes in Legendre polynomials. Writing $\bar{\varphi}_j(\mu) = A_j(\mu) \varphi_j(\mu)$, the expansion is $\bar{\varphi}_j(\mu) = \sum_{l=0}^{\infty} P_l(\mu) \bar{\varphi}_{j,l}$, with components $\bar{\varphi}_{j,l} = (2l+1) \langle P_l(\mu) \bar{\varphi}(\mu) \rangle$. Using that

$$\int_0^1 d\mu \mu (\bar{\varphi}_2^s \bar{\varphi}_1^a - \bar{\varphi}_1^s \bar{\varphi}_2^a) = \sum_{l=0}^{\infty} \frac{(-1)^l (l+1)}{(2l+1)(2l+3)} (\bar{\varphi}_{2,l} \bar{\varphi}_{1,l+1} - \bar{\varphi}_{1,l} \bar{\varphi}_{2,l+1}), \quad (17)$$

we can bring Eq. (5) into the form $J_c = \sum_{l=0}^{\infty} J_{c;l,l+1}$.

ACKNOWLEDGEMENTS

The authors would like to thank Juha Kopu (in particular in the earlier stages of this work) and Gerd Schön for valuable contributions, Anna Posazhennikova for helpful comments on the manuscript, and Teun Klapwijk for communications in relation to experiment [2]. T.L. acknowledges financial support from the Alexander von Humboldt Foundation. Supplementary Information accompanies this paper.

-
- [1] Chakhalian, J. *et al.* Magnetism at the interface between ferromagnetic and superconducting oxides. *Nature Physics* **2**, 244-248 (2006).
- [2] Keizer, R.S. *et al.* A spin triplet supercurrent through the half-metallic ferromagnet CrO_2 . *Nature* **439**, 825-827 (2006).
- [3] Volkov, A. F., Bergeret, F. S. & Efetov, K. B. Odd Triplet Superconductivity in Superconductor-Ferromagnet Multilayered Structures. *Phys. Rev. Lett.* **90**, 117006 (2003).
- [4] Asano, Y., Tanaka, Y. & Golubov, A. Josephson Effect due to Odd-frequency Pairs in Diffusive Half Metals. Unpublished, cond-mat/0609566 (2006).
- [5] Eschrig, M., Kopu, J., Cuevas, J. C. & Schön, G. Theory of Half-Metal/Superconductor Heterostructures. *Phys. Rev. Lett.* **90**, 137003 (2003).
- [6] Tokuyasu, T., Sauls, J. A. & Rainer, D. Proximity effect of a ferromagnetic insulator in contact with a superconductor. *Phys. Rev. B* **38**, 8823-8833 (1988).
- [7] Bergeret, F. S., Volkov, A. F. & Efetov, K. B. Odd triplet superconductivity and related phenomena in superconductor-ferromagnet structures. *Rev. Mod. Phys.* **77**, 1321-1373 (2005).
- [8] Eilenberger, G. Transformation of Gorkov's Equation for Type II Superconductors into Transport-Like Equations. *Z. Phys.* **214**, 195-213 (1968).
- [9] Larkin, A. I. & Ovchinnikov, Y. N. Quasiclassical Method in Theory of Superconductivity. *Zh. Eksp. Teor. Fiz.* **55**, 2262-& (1968), [Sov. Phys. JETP **28**, 1200-& (1969)].
- [10] Klapwijk, T. M. private communications.
- [11] Anderson, P. W. Theory of dirty superconductors. *J. Phys. Chem. Solids* **11**, 26-30 (1959).
- [12] Abrikosov, A. A. & Gor'kov, L. P. Superconducting alloys at finite temperatures. *Zh. Eksp. Teor. Fiz.* **36**, 319-320 (1959) [Sov. Phys. JETP **9**, 220-221 (1959)].
- [13] Larkin, A. I. Vector pairing in superconductors of small

dimensions. *Pis'ma Zh. Eksp. Teor. Fiz.* **2**, 205-209 (1965) [Sov. Phys. JETP Lett. **2**, 130-133 (1965)].

- [14] Buzdin, A. I., Bulaevskii, L. N. & Panyukov, S. V. Critical-current oscillations as a function of the exchange field and thickness of the ferromagnetic metal (F) in an S-F-S Josephson junction. *Pis'ma Zh. Eksp. Teor. Fiz.* **35**, 147-148 (1982) [Sov. Phys. JETP Lett. **35**, 178-180 (1982)].
- [15] Braude, V. & Nazarov, Yu. V. Fully developed triplet proximity effect. Unpublished, cond-mat/0610037 (2006).
- [16] Eschrig, M. *et al.* Symmetries of Pairing Correlations in Superconductor-Ferromagnet Nanostructures. To be published in *J. Low Temp. Phys.* ; cond-mat/0610212 (2006).
- [17] Lewis, S. P., Allen, P. B. & Sasaki, T. Band structure and transport properties of CrO_2 . *Phys. Rev. B* **55**, 10253-10260 (1997).

SUPPLEMENTARY MATERIAL

In Supplementary Fig. 1 we show solutions of the integral equations in the superconductor, Eqs. (11)-(12), and in the half metal, Eq. (13), for several impurity concentrations ranging from the ballistic limit to the diffusive limit. In the left panels we vary the superconducting mean free path ℓ_S , and in the right panels the half metal mean free path ℓ_H for fixed ℓ_S . In the inset we also show the induced spin polarization in the superconductors. It is calculated from the the diagonal part of the Green's function, given by

$$g_{zj}(x) = -\pi \frac{|\Delta|^2 \vartheta_j}{\varepsilon_n^2 + |\Delta|^2} \text{sgn}(\varepsilon_n) \varphi_{0j}^s(x). \quad (18)$$

There is, consequently, a surface spin polarization in the superconductor, that in the clean limit is given by $\langle g_{zj}(x) \rangle = -\pi |\Delta|^2 \langle \vartheta_j e^{-|x-x_j|/\xi_S |\mu|} \rangle / 2(\varepsilon_n^2 + |\Delta|^2)$. The induced spin magnetization is then

$$\delta M_z(x) = 2\mu_B N_S T \sum_{\varepsilon_n} \langle g_{zj}(x) \rangle, \quad (19)$$

where μ_B is the Bohr magneton and N_S is the density of states in the superconductor.

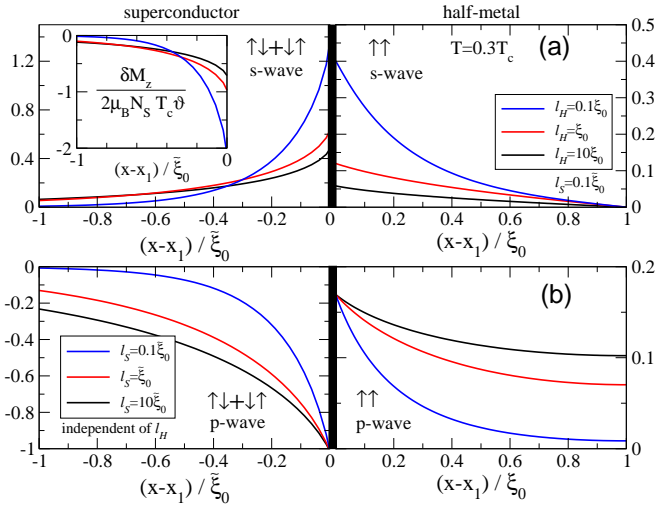


FIG. 1: (Supplementary Figure) Spatial dependences of pairing amplitudes in the superconductor and in the half metal (length $L = 2\xi_0$, only left half shown) for a π -junction. The odd-frequency s -wave triplet amplitude is shown in the upper panel, the even-frequency p -wave triplet amplitude in the lower panel. In the inset we show the induced spin polarization of quasiparticles near the interface in the superconductor. The triplet amplitudes in the superconductor are $m = 0$ with respect to the superconducting quantization axis, and in the half metal are equal-spin $m = 1$ amplitudes with respect to the magnetization axis \mathbf{M} . The quantization axis in the superconductor can be slightly misaligned with respect to that in the half metal as result of the breaking of spin-rotation symmetry around \mathbf{M} at the interface.